


NANO EXPRESS

Open Access



# Electric-Controlled Valley Pseudomagnetoconductance in Graphene with Y-Shaped Kekulé Lattice Distortion

Qing-Ping Wu<sup>1</sup>, Lu-Lu Chang<sup>1</sup>, Yu-Zeng Li<sup>1</sup>, Zheng-Fang Liu<sup>1\*</sup>  and Xian-Bo Xiao<sup>2</sup>

## Abstract

We propose a new method for regulating valley pseudomagnetoconductance in ballistic graphene-based valley field-effect transistors by taking into account the Y-shaped Kekulé lattice distortion and electric barrier. The device involves valley injection and valley detection by ferromagnetic-strain source and drain. The valley manipulation in the channel is achieved via the Y-shaped Kekulé lattice distortion and electric barrier. The central mechanism of these devices lies on Y-shaped Kekulé lattice distortion in graphene can induce a valley precession, thus controlling the valley orientation of channel electrons and hence the current collected at the drain. We found that the tuning external bias voltage makes the valley pseudomagnetoconductance oscillate between positive and negative values and colossal tunneling valley pseudomagnetoconductance of over 30,000% can be achieved. Our results suggest that the synergy of valleytronics and digital logics may provide new paradigms for valleytronic-based information processing and reversible computing.

**Keywords:** Pseudomagnetoconductance, Y-shaped Kekulé lattice, Graphene

## Introduction

Graphene, being a two-dimensional sheet of carbon atoms, which have excellent carrier mobility and offers the thinnest possible channel for utilizing to design of metal-oxide-semiconductor field-effect transistors [1]. Semenov have proposed a spin field-effect transistor by utilizing a graphene layer as the channel [2], which involves spin injection and spin detection by ferromagnetic source and drain, and the spin manipulation in the channel is achieved via electrical control of the electron exchange interaction with a ferromagnetic gate. In addition, Rashba spin-orbit interaction is another promising tool for the spin control in graphene [3]. The Rashba spin-orbit interaction can induces a spin precession, thus controlling the spin orientation of channel electrons. The spin field-effect transistors also inspired many important research ideas, such as giant magnetoconductance and tunnel magnetoconductance [3, 4]. The giant magnetoconductance and tunnel

magnetoconductance can be applied in digital storage and magnetic sensor technologies.

On the other hand, Dirac electrons in graphene possess extra valley degree of freedom besides the conventional charge and spin counterparts. Owing to the large momentum difference between the two valleys and the suppression of the intervalley scattering in clean graphene samples [5–7], the valley degree of freedom is believed to exert the same effect as the electron spin in carrying and manipulating information, which leads to a new discipline rising as valleytronics. In analog of spin field-effect transistor, valley field-effect transistor is also theoretically proposed in graphene [8], which consists of a quantum one dimension channel of gapped graphene sandwiched between two armchair graphene nanoribbons (source and drain); then, side gate electric field is applied to the channel and modulates the valley polarization of carriers due to the valley-orbit interaction, thus controlling the amount of current collected at the drain. However, due to the fact that the valley coupling in graphene has not become a physical reality for a long time, there are few further studies based on the valley field-effect transistors of graphene and related studies. Recent experiments by Gutierrez et al. [9] have revealed an unusual Y-shaped Kekulé(Kek-Y)

\*Correspondence: [lzhengfang@ecjtu.edu.cn](mailto:lzhengfang@ecjtu.edu.cn)

<sup>1</sup>Department of Applied Physics, East China Jiaotong University, Nanchang 330013, China

Full list of author information is available at the end of the article

bond texture in the honeycomb lattice on a graphene-copper superlattice, where one of six carbon atoms in each superlattice unit cell has no copper atoms below it and acquires a shorter nearest-neighbor bond. Further, Gamayun has shown that the Kek-Y bond texture offers a way for a momentum-controlled valley precession [10]. Beenakker et al. [11] showed that the Kek system can bring out a valley flip effect via the Andreev-like reflection. Recently Wang et al. [12] found that the C-C bond-length modulation of the Kekulé lattice that keeps the inversion symmetry of the system can be used to manipulate the valley degree of freedom in a similar way to the exchange field precessing spin. This makes it possible to design a new type of valley field-effect transistor in graphene. Moreover, there is no report on the combined effects of the Kek-Y lattice distortion on the valley pseudomagnetoconductance in graphene. Valley pseudomagnetoconductance [13, 14] is analogous to the magnetoconductance in magnetic tunnel junction [15] where the magnitude of the spin current depends on the magnetic orientation of the electrodes [4].

## Methods

In this work, we propose a new type of valley field-effect transistors (VFETs) for graphene-based electron. The device design assumes a ferromagnetic-strain (FM-S) source/drain for valley polarized injection/detection, which resembles conventional spin transistor (see Fig. 1a).

Valley rotation in the graphene channel relies on Kek-Y graphene superlattice [10–12], which can be achieved by a superlattice of graphene grown epitaxially onto Cu(111), with the copper atoms in registry with the carbon atoms [9]. However, copper atoms are lacking under some carbon atoms, resulting in some periodic copper atom vacancies appearing below graphene. Such substrate atom vacancy leads to three neighboring bonds being contracted. Here, we use  $\delta t$  to represent the energy modification to the electron's hopping corresponding to these three bonds. We assume that the ferromagnetic graphene is made of the same FM metal stripe. The two magnetizations of the source and drain are directed along the current direction (the  $x$  axis), which can be in either the parallel (P) or the antiparallel (AP) alignment, with the help of an external in-plane magnetic field. In the Landau gauge, the magnetic vector potential arising from the fringe field has the form [16, 17]  $A(r) = A_y(x)\vec{y}$  with  $A_y(x) = A_y[\Theta(-x) \pm \Theta(x-L)]$ , where the plus(minus) sign corresponds to the P(AP) configuration of magnetizations,  $\Theta(x)$  is the Heaviside step function. On the other hand, we assume that the same strain are applied on source and drain of the VFETs, which can be induced by a tension on the substrate of the graphene [18]. The elastic deformation can be treated as a perturbation to the hopping amplitudes and acts as a gauge potential  $A_S(r)$ . The tension is set along the  $x$  direction, in this case,  $A_S(r)$

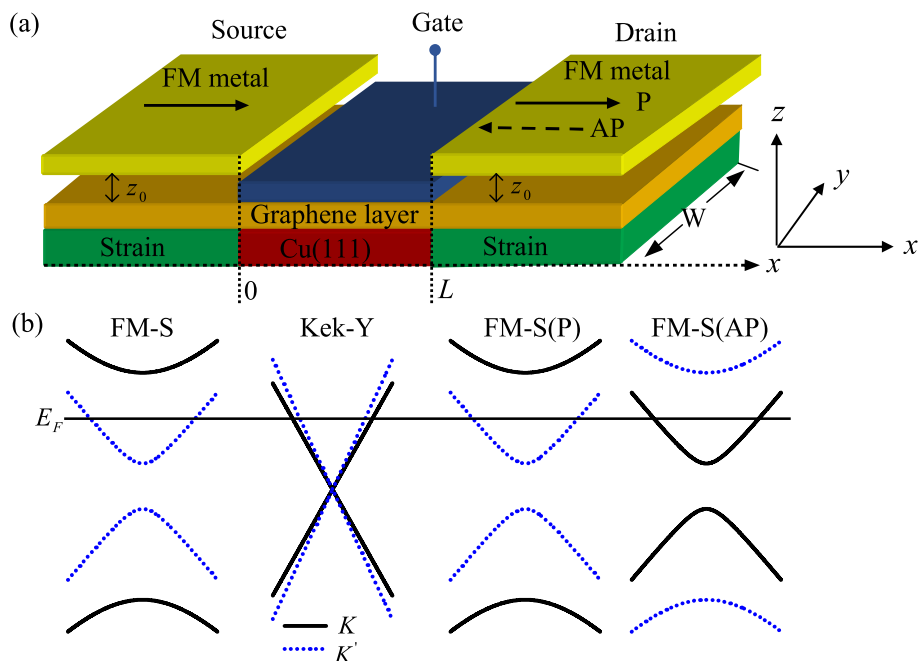


**Fig. 1** **a** Schematic illustration of the VFET utilizing a graphene channel with Kek-Y lattice distortion and a gate bias, which controls the valley orientation of channel electrons. The source and drain are FM-S graphene, which inject and detect electrons in a specific polarization. Where  $z_0$  is the distance between the graphene layer and the FM stripe.  $L$  is the channel length,  $W$  is the width of the graphene sample in the  $y$  direction, and  $W \gg L$ . **b** Band structure near Dirac points. The horizontal line denotes the Fermi energy (color online)

uniform along the  $y$  axis [16]. For definiteness, we take a typical smooth profile of its  $y$  component as  $A_S(x) = A_S [\Theta(-x) + \Theta(x-L)]$ , where  $A_S$  is the amplitude. In addition, a electric barrier are also applied in the Kek-Y lattice region, which can be tuned by external bias voltage.

The low-energy excitation quasiparticles propagation in the VFETs with Kek-Y graphene superlattices can be described by the following single particle Hamiltonian [10–12]

$$H = v_F(\mathbf{P} \cdot \sigma) + v_\tau(\mathbf{P} \cdot \tau)\Theta(x)\Theta(L-x) + U\sigma_0\tau_0\Theta(x)\Theta(L-x) + A_M(x)\sigma_y + \tau_z A_S(x)\sigma_y. \quad (1)$$

Here,  $\sigma$  and  $\tau$  are the Pauli matrices for the sublattice and the valley, respectively.  $\mathbf{P} = (p_x, p_y)$  is the momentum of massless Dirac electrons,  $\tau_z = \pm 1$  for  $K$  and  $K'$  valleys,  $v_F = 10^6$  m/s is the velocity of Dirac electrons in the pristine graphene, and  $v_\tau \simeq v_F \delta t / 3t$  is the velocity modification term from the bond contraction effect in the Kek-Y lattice [12], where  $t$  is the hopping energy between the nearest neighboring sites for pristine graphene.  $U$  is the gate-tunable potential barrier.  $A_M(x) = e v_F A_y(x)$  [19]. The eigenvalues of the Hamiltonian in the graphene with Kek-Y lattice distortion and electric barrier are given by

$$E_{\alpha,\beta} = U + \alpha(\hbar v_F + \beta \hbar v_\tau) \sqrt{k_{x\beta}^2 + k_y^2}. \quad (2)$$

Here,  $\alpha = +1(-1)$  specifies the conduction (valence) band.  $\beta = \pm 1$  denotes the two valley-split subbands of the conduction and valence bands. Due to the translational invariance in the  $y$  direction, the transverse wave vector  $k_y$  is conserved. The eigenstates in the graphene with the homogeneous Kek-Y lattice distortion are characterized by  $\Psi_\beta^\pm(k_{x\beta}, k_y) = \frac{1}{N_\beta} (1, P_\beta^\pm, Q_\beta^\pm, R_\beta^\pm)^T$ , where  $N_\beta$  is the normalization constant  $N_\beta = (1 + P_\beta^2 + Q_\beta^2 + R_\beta^2)^{\frac{1}{2}}$  and  $P_\beta^\pm, Q_\beta^\pm$ , and  $R_\beta^\pm$  are functions defined as follows:

$$\begin{aligned} P_\beta^\pm &= \frac{(E-U)^2 + (\hbar^2 v_F^2 - \hbar^2 v_\tau^2)(k_{x\beta}^2 + k_y^2)}{2(E-U)\hbar v_F(\pm k_{x\beta} - ik_y)}, \\ Q_\beta^\pm &= \frac{(E-U)^2 - (\hbar^2 v_F^2 - \hbar^2 v_\tau^2)(k_{x\beta}^2 + k_y^2)}{2(E-U)\hbar v_\tau(\pm k_{x\beta} - ik_y)}, \\ R_\beta^\pm &= \frac{(E-U)^2 - (\hbar^2 v_F^2 + \hbar^2 v_\tau^2)(k_{x\beta}^2 + k_y^2)}{2\hbar^2 v_F v_\tau(\pm k_{x\beta} - ik_y)^2}. \end{aligned} \quad (3)$$

The transmission probability from  $K'$  valley to  $K(K')$  valley  $T_{K',K(K')}$  can be calculated using the transfer matrix technique [20]. According to the Landauer-Büttiker formula, the valley-dependent conductance is given by [21]:

$$G_{K',K(K')} = G_0 \int_{-\frac{\pi}{2}}^{\frac{\pi}{2}} T_{K',K(K')} \cos(\phi_0) d\phi_0. \quad (4)$$

Here  $G_0 = 2e^2 W / (v_F \pi^2 \hbar^2) |E|$ ,  $W$  is the width of the graphene sample in the  $y$  direction, and  $\phi_0$  is the incident angle with respect to the  $x$  direction.

Before proceeding with the calculations, we discuss the band structure with  $k_y = 0$ , as shown in Fig. 1b. In the FM-S source region, the energy band of graphene is written as  $E = \alpha \sqrt{(\hbar v_F k_x)^2 + (A_M + \tau_z A_S)^2}$ . One can find that the valley degenerate is lift and different gaps are induced at the  $K$  and  $K'$  points because the total vector potential  $A_M + A_S$  acting on  $K$  electrons is higher than the total vector potential  $|A_M - A_S|$  acting on for  $K'$  electrons [19]. This indicates that only  $K'$  electrons can pass through the FM-S source region when the incident energy is located in  $|A_M - A_S| < E < A_M + A_S$  [22, 23]. Similarly, in the FM-S drain region, the energy band of graphene can be written as  $E = \alpha \sqrt{(\hbar v_F k_x)^2 + (\pm A_M + \tau_z A_S)^2}$ , where the  $\pm$  sign corresponds to the P and AP configuration of magnetizations. So only  $K'$  electrons are detected in the P structure and only  $K$  electrons are detected in the AP structure when the Fermi energy locates at the range of  $[|A_M - A_S|, A_M + A_S]$ . In the graphene channel, the valley degenerate is also lift, but there is an important difference. In contrast to the lead case, where the phases of  $K$  and  $K'$  components evolve with the same wave vector [i.e.,  $k = E/\hbar v_F$ ], now, they evolve separately with different wave vectors ( $k_+ = (E - U)/(\hbar v_F + \hbar v_\tau)$  and  $k_- = (E - U)/(\hbar v_F - \hbar v_\tau)$ ) due to the Kek-Y graphene superlattices mixing the valley (see Eq. 2). This leads to the valley precession of channel electrons in the valley space [12]. The valley precession in graphene is the basis for the valley field effect transistor [8]. And the valley precession can also be characterized by a valley pseudomagneto-resistance (VPMR) in the FM-S/Kek-Y/FM-S junctions, analogous to the magnetoresistance in graphene-based quantum tunneling junctions with the spin-orbit interaction [4], which is defined as  $VPMR = \frac{G_P - G_{AP}}{G_P}$ , where  $G_P$  and  $G_{AP}$  represent the conductance in P and AP configurations, respectively, and  $G_P = G_{K',K'}$ ,  $G_{AP} = G_{K,K}$ . The magnitude of the valley current depends on the magnetic orientation of the source and drain in our considered device.

### Numerical Results and Discussions

In the following, we present the numerical results for the FM-S/Kek-Y/FM-S junction in graphene. Throughout the paper, we set channel length  $L = 207$  nm, and restrict the Fermi energy  $20 \text{ meV} < E < 140 \text{ meV}$ , assumed it satisfying  $|A_M - A_S| < E < A_M + A_S$ . Figure 2a and b show the calculated results of tunneling conductance and VPMR as a function of  $v_t$  with Fermi energy  $E = 80 \text{ meV}$  and rectangle potential barrier  $U = -10 \text{ meV}$ . We can find that  $G_P$  and  $G_{AP}$  have the same oscillation periods but the inverse phases. Therefore, the VPMR oscillates with increase of  $v_t$  and the negative value VPMR can appear.

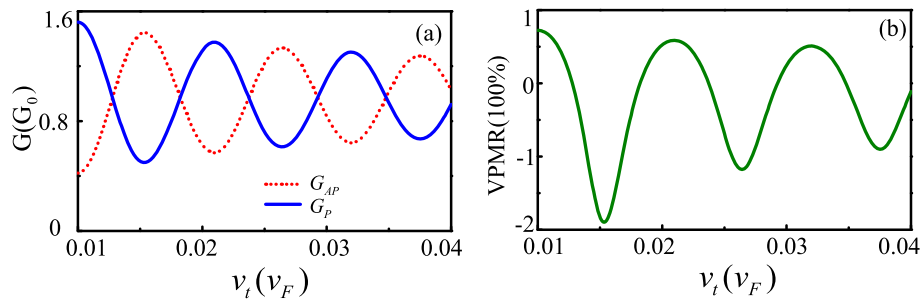


**Fig. 2** Conductance  $G_{P,AP}$  and VPMR versus  $v_t$  at  $L = 207$  nm,  $E = 80$  meV and  $U = -10$  meV (color online)

Those phenomena are similar to the case of the magnetoresistance in ballistic graphene-based quantum tunneling junctions with the spin-orbit interaction [4]. The oscillation characters of the conductance of  $G_P$  and  $G_{AP}$  can be explained by the phase difference between the two valley components. When the incident angle  $\phi_0 = 0$ , the phase shift is given by:  $\Delta\theta = (k_{x+} - k_{x-})L = -\frac{2(E-U)v_t}{\hbar(v_F^2 - v_t^2)}L$ .  $\Delta\theta$  determines the orientation of valley polarization before the electron enters the drain, relative to that of the drain state [8]. For  $\Delta\theta = \pm 2n\pi$ ,  $n = 1, 2, 3 \dots$ , the two polarizations are aligned, leading to the conductance  $G_P$  maximum and VPMR a high positive value (as seen in  $v_t = 0.022, 0.033$ ). On the other hand, for  $\Delta\theta = \pm(2n + 1)\pi$ ,  $n = 0, 1, 2 \dots$ , they are orthogonal to each other, leading to the conductance  $G_{AP}$  minimum and VPMR negative (as seen in  $v_t = 0.0167, 0.027, 0.038$ ).

The conductance and VPMR are not only oscillation functions of the hopping-energy modification, they also oscillate with Fermi energy and the effective barrier potential since  $\Delta\theta$  scales are also linear with the Fermi energy and the potential barrier  $U$ . Figure 3a and b show the conductance as a function of Fermi energy and the effective barrier potential, respectively. The corresponding VPMR are given in Fig. 3c and d. They all show oscillation characteristics varying with  $E$  and  $U$  value, even when the effective barrier potential  $U$  is greater than Fermi energy  $E$ . The physical origin for such a phenomenon is related to the Klein tunneling [12]. Although there are similar oscillation phenomena of conductance and VPMR for increased  $E$  and  $U$ , some differences can be also found. As  $E$  increases, the difference between  $G_P$  and  $G_{AP}$  conductance becomes smaller and smaller,

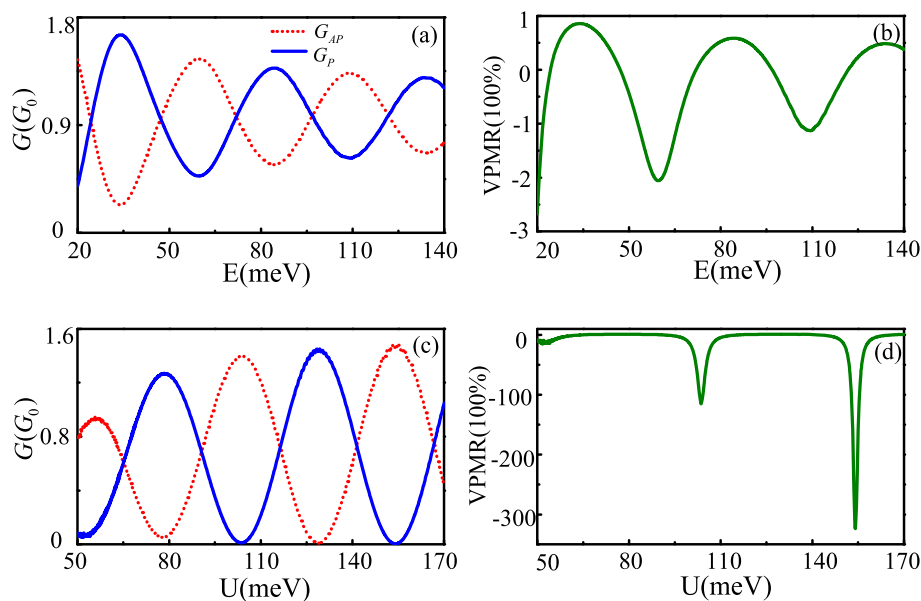


**Fig. 3** Conductance  $G_{P,AP}$  (a, c) and VPMR (b, d) as functions of the Fermi energy and the electric barrier at  $L = 207$  nm,  $v_t = 0.02v_F$ . The other parameters are  $U = -10$  meV for a and c,  $E = 80$  meV for b and d (color online)

which lead the oscillation amplitude of VPMR to become decreased with the increase of Fermi energy. While under the condition  $\Delta\theta = \pm n\pi$  is satisfied, the difference between  $G_P$  and  $G_{AP}$  is greater with increasing of  $U$ , especially in some location, the  $G_P$  and  $G_{AP}$  conductance presents switching characteristics. The characters are more desirable for the application of VPMR. Remarkably, the observed maximum value of VPMR is over 30,000% at small  $E$ . This value greatly exceeds MR of  $\sim 175\%$  in the ballistic graphene-based quantum tunneling junctions with the spin-orbit interaction [4] and the pseudomagnetoconductance of  $\sim 100\%$  in bilayer graphene controlled by external gates [24], which is even larger than the VPMR of  $\sim 10000\%$  in a merging Dirac cones system [13].

## Conclusions

In conclusion, we proposed a type of valley field-effect transistors for graphene-based electron and studied the valley pseudomagnetoconductance through it. We have shown that the oscillation feature of valley pseudomagnetoconductance not only related to the hopping-energy modification and Fermi energy, but also can be tuned largely by the effective barrier potential. The valley pseudomagnetoconductance tuned by external bias voltage benefits the valley field-effect transistor device, and we anticipate that the electric controlled valley quantum devices proposed here can play a role in quantum and quantum-classical hybrid computers.

Further research could involve the different strain (uniaxial vs. biaxial) tunable the valley scattering of electrons and transport in our proposed graphene-based valley field-effect transistors since the strain is useful to control the degree of intervalley scattering in Kekulé patterns [25]. Then, other two-dimensional materials ( $\text{MoS}_2$ ,  $\text{WS}_2$ ,  $\text{WSe}_2$ , etc.) analogs in graphene can also provide an interesting platform for other two-dimensional material-based valley field-effect transistors with Y-shaped Kekulé lattice distortion.

## Abbreviations

AP: Antiparallel; FM-S: Ferromagnetic-strain; Kek-Y: Y-shaped Kekulé; P: Parallel; VFETs: Valley field-effect transistors; VPMR: Valley pseudomagnetoconductance

## Acknowledgements

This work is supported by the National Natural Science Foundation of China (grant nos. 11764013, 11864012, and 11664019).

## Authors' Contributions

QPW conceived the research work. LLC and YZL carried out the computation. QPW, ZFL, and XBK analyzed the results and wrote the manuscript. All the authors read and approved the final manuscript.

## Funding

This work is supported by the National Natural Science Foundation of China (grant nos. 11764013, 11864012, and 11664019).

## Availability of Data and Materials

The datasets supporting the conclusions of this article are included within the article.

## Competing Interests

The authors declare that they have no competing interests.

## Author Details

<sup>1</sup>Department of Applied Physics, East China Jiaotong University, Nanchang 330013, China. <sup>2</sup>School of Computer Science, Jiangxi University of Traditional Chinese Medicine, Nanchang 330004, China.

Received: 22 October 2019 Accepted: 4 February 2020

Published online: 19 February 2020

## References

- Schwierz F (2010) Graphene transistors. *Nat Nanotechnol* 5(7):487
- Semenov Y, Kim K, Zavada J (2007) Spin field effect transistor with a graphene channel. *Appl Phys Lett* 91(15):153105
- Beiranvand R, Hamzehpour H (2019) Tunable magnetoresistance in spin-orbit coupled graphene junctions. *J Magn Magn Mater* 474:111–117
- Bai C, Wang J, Jia S, Yang Y (2010) Spin-orbit interaction effects on magnetoresistance in graphene-based ferromagnetic double junctions. *Appl Phys Lett* 96(22):223102
- Morpurgo A, Guinea F (2006) Intervalley scattering, long-range disorder, and effective time-reversal symmetry breaking in graphene. *Phys Rev Lett* 97(19):196804
- Morozov SV, Novoselov KS, Katsnelson MI, Schedin F, Ponomarenko LA, Jiang D, Geim AK (2006) Strong suppression of weak localization in graphene. *Phys Rev Lett* 97:016801
- Chen JH, Cullen WG, Jang C, Fuhrer MS, Williams ED (2009) Defect scattering in graphene. *Phys Rev Lett* 102:236805
- Lee MK, Lue NY, Wen CK, Wu G (2012) Valley-based field-effect transistors in graphene. *Phys Rev B* 86(16):165411
- Gutiérrez C, Kim CJ, Brown L, Schiros T, Nordlund D, Lochocki EB, et al (2016) Imaging Chiral symmetry breaking from Kekulé bond order in graphene. *Nat Phys* 12(10):950
- Gamayun O, Ostroukh V, Gnezdilov N, Adagideli İ, Beenakker C (2018) Valley-momentum locking in a graphene superlattice with y-shaped Kekulé bond texture. *New J Phys* 20(2):023016
- Beenakker CWJ, Gnezdilov NV, Dresselhaus E, Ostroukh VP, Herasymenko Y, Adagideli İ, Tworzydło J (2018) Valley switch in a graphene superlattice due to pseudo-Andreev reflection. *Phys Rev B* 97:241403(R)
- Wang JJ, Liu S, Wang J, Liu JF (2018) Valley-coupled transport in graphene with y-shaped Kekulé structure. *Phys Rev B* 98(19):195436
- Ang YS, Yang SA, Zhang C, Ma Z, Ang LK (2017) Valleytronics in merging Dirac cones: all-electric-controlled valley filter, valve, and universal reversible logic gate. *Phys Rev B* 96(24):245410
- Wu Z, Zhai F, Peeters F, Xu H, Chang K (2011) Valley-dependent Brewster angles and Goos-Hänchen effect in strained graphene. *Phys Rev Lett* 106(17):176802
- Zhang YT, Jiang H, Sun Qf, Xie X (2010) Spin polarization and giant magnetoresistance effect induced by magnetization in zigzag graphene nanoribbons. *Phys Rev B* 81(16):165404
- Zhai F, Zhao X, Chang K, Xu H (2010) Magnetic barrier on strained graphene: a possible valley filter. *Phys Rev B* 82(11):115442
- Moldovan D, Masir MR, Covaci L, Peeters F (2012) Resonant valley filtering of massive Dirac electrons. *Phys Rev B* 86(11):115431
- Teague M, Lai A, Velasco J, Hughes C, Beyer A, Bockrath M, et al (2009) Evidence for strain-induced local conductance modulations in single-layer graphene on SiO<sub>2</sub>. *Nano Lett* 9(7):2542–2546
- Song Y, Zhai F, Guo Y (2013) Generation of a fully valley-polarized current in bulk graphene. *Appl Phys Lett* 103(18):183111
- Wu QP, Liu ZF, Chen AX, Xiao XB, Zhang H, Miao GX (2017) Valley precession and valley polarization in graphene with inter-valley coupling. *J Phys-Condens Matter* 29(39):395303
- Büttiker M, Imry Y, Landauer R, Pincus S (1985) Generalized many-channel conductance formula with application to small rings. *Phys Rev B* 31(10):6207

22. Wu QP, Liu ZF, Chen AX, Xiao XB, Liu ZM (2016) Full valley and spin polarizations in strained graphene with Rashba spin orbit coupling and magnetic barrier. *Sci Rep* 6:21590
23. Wu QP, Liu ZF, Chen AX, Xiao XB, Miao GX (2017) Pure valley and spin polarization current in ferromagnetic graphene junction. *J Appl Phys* 121(5):053906
24. San-Jose P, Prada E, McCann E, Schomerus H (2009) Pseudospin valve in bilayer graphene: towards graphene-based pseudospintronics. *Phys Rev Lett* 102(24):247204
25. Andrade E, Carrillo-Bastos R, Naumis GG (2019) Valley engineering by strain in Kekulé-distorted graphene. *Phys Rev B* 99:035411

### **Publisher's Note**

Springer Nature remains neutral with regard to jurisdictional claims in published maps and institutional affiliations.

**Submit your manuscript to a SpringerOpen<sup>®</sup> journal and benefit from:**

- ▶ Convenient online submission
- ▶ Rigorous peer review
- ▶ Open access: articles freely available online
- ▶ High visibility within the field
- ▶ Retaining the copyright to your article

---

Submit your next manuscript at ▶ [springeropen.com](https://www.springeropen.com)

---